AGU100 ADVANCING EARTH AND SPACE SCIENCE

Geophysical Research Letters

RESEARCH LETTER
10.1029/2019GL083703

Seasonal Prediction Potential for Springtime Dustiness in the United States

Bing Pu[1,2,3], Paul Ginoux[2], Sarah B. Kapnick[2], and Xiaosong Yang[2,4]

[1]Atmospheric and Oceanic Sciences Program, Princeton University, Princeton, NJ, USA, [2]NOAA Geophysical Fluid Dynamics Laboratory, Princeton, NJ, USA, [3]Department of Geography and Atmospheric Science, The University of Kansas, Lawrence, KS, USA, [4]Cooperative Programs for the Advancement of Earth System Science, University Corporation for Atmospheric Research, Boulder, CO, USA

Key Points:
- A regression model and ensembles from a seasonal prediction model initialized on 1 December are used to predict springtime dustiness
- About 71% of the variances of dustiness over the Great Plains and 63% over the southwestern United States from 2004 to 2016 are captured
- Springtime climatic factors play a more important role in variations in spring dustiness than wintertime factors

Supporting Information:
- Supporting Information S1

Correspondence to:
B. Pu,
bpu@ku.edu

Citation:
Pu, B., Ginoux, P., Kapnick, S., & Yang, X. (2019). Seasonal prediction potential for springtime dustiness in the United States. *Geophysical Research Letters*, *46*. https://doi.org/10.1029/2019GL083703

Received 13 MAY 2019
Accepted 12 JUL 2019
Accepted article online 19 JUL 2019

Abstract

Most dust forecast models focus on short, subseasonal lead times, that is, 3 to 6 days, and the skill of seasonal prediction is not clear. In this study we examine the potential of seasonal dust prediction in the United States using an observation-constrained regression model and key variables predicted by a seasonal prediction model developed at National Oceanic and Atmospheric Administration Geophysical Fluid Dynamics Laboratory, the Forecast-Oriented Low Ocean Resolution (FLOR) model. Our method shows skillful predictions of spring dustiness 3 to 6 months in advance. It is found that the regression model explains about 71% of the variances of dust event frequency over the Great Plains and 63% over the southwestern United States in March-May from 2004 to 2016 using predictors from FLOR initialized on 1 December. Variations in springtime dustiness are dominated by springtime climatic factors rather than wintertime factors. Findings here will help development of a seasonal dust prediction system and hazard prevention.

Plain Language Summary

Severe dust storms reduce visibility and cause breathing problems and lung diseases, affecting public transportation and safety. Reliable forecasts for dust storms and overall dustiness are therefore important for hazard prevention and resource planning. Most dust forecast models focus on short-time forecasts extending out only a few days. The capability of seasonal dust prediction in the United States is not clear. Here we use a statistical model and precipitation, surface wind, and ground surface bareness from a seasonal prediction model driven by observational information on 1 December to predict dustiness over major dusty regions in the United States in spring. It is found that our method can largely capture the year-to-year variations in dustiness over the Great Plains during March-April-May and partially over the southwestern United States. The finding here will help the development of a more reliable seasonal dust prediction system in the future.

1. Introduction

Mineral dust plays an important role in the climate system and local environment. Dust particles absorb and scatter both solar and terrestrial radiation, thus affecting the local radiative budget and regional hydroclimate. For instance, dust is found to amplify severe droughts in the United States by increasing atmospheric stability (e.g., Cook et al., 2008, 2009, 2013), to modulate the North American monsoon by heating the lower troposphere (Zhao et al., 2012), and to accelerate snow melting and perturb runoff over the Upper Colorado River Basin by its deposition on snow (e.g., Painter et al., 2010, 2018).

Dust particles also affect air quality. Over the southwestern and central United States, fine dust (with an aerodynamic diameter < 2.5 μm) is an important component of total particulate matter 2.5 ($PM_{2.5}$) mass, contributing about 20–50% to total $PM_{2.5}$ mass in the southwestern and central United States in spring and summer (Hand et al. 2017).

Severe dust storms degrade visibility and cause breathing problems and lung diseases, affecting public transportation and health (e.g., Giannadaki et al., 2014; Goudie, 2009; Kolivras & Comrie, 2004; Schweitzer et al., 2018). It is found that dust storms are associated with increases in nonaccidental and cardiovascular mortality in the United States (Crooks et al., 2016). Tong et al. (2017) found that incidences of Valley fever in Arizona are associated with dust storms.

Reliable forecasts for dust storms and overall dustiness are therefore important for public safety and health and resource planning. Some regional or global models provide dust forecasts for 3 to 6 days. For instance, the Navy Aerosol Analysis and Prediction System (NAAPS) is an operational global aerosol model (Christensen, 1997; Reid et al., 2009; Witek et al., 2007) using the meteorological analysis and forecast variables from the Navy's Operational Global Analysis and Prediction System (NOPAPS) to provide 6-day forecasts of dust, sulfate, and other aerosols (Rubin et al., 2016; Westphal et al., 2009). SKIRON/Eta system developed at the University of Athens (Kallos et al., 2006) provides operational dust and weather forecasts over the Mediterranean region for 3 to 5 days. The Barcelona Supercomputing Center (BSC)-dust model is fully embedded in the non-hydrostatic multiscale model developed at the National Centers for Environmental Prediction to provide regional or global short to medium range (~3 days) dust forecasts (Haustein et al., 2012; Pérez et al., 2011).

Dust forecast models are either online coupled with or offline driven by weather forecast models, which provide necessary meteorological conditions for the dust scheme to simulate the life cycle of the dust. Longer-lead predictions, that is, seasonal dust prediction, are less studied. Different from weather forecast, seasonal prediction is not only an initial-condition problem but also a boundary-condition problem that is somewhat similar to decadal prediction or climate change projections (Doblas-Reyes et al., 2013).

There are a few studies of seasonal dust prediction in Asia through statistical methods (Gao et al., 2010; Sohn, 2013). For instance, Gao et al. (2009) examined the potential of using previous annual mean precipitation to predict subsequent springtime dust storm frequency in the Inner Mongolia region as precipitation can influence soil moisture and vegetation growth. Over sub-Saharan Africa, zonal wind speed in November-December has been used to predict dust related Meningitis incidence in January-May (Pérez García-Pando et al., 2014). To the best of our knowledge, however, few studies investigated seasonal dust prediction in the United States or used dynamic seasonal prediction models for dust prediction.

Here we examine the potential of seasonal prediction of dustiness in the United States by using an observation-constrained regression model (Pu & Ginoux, 2017) and meteorological fields (as predictors) from a coupled global seasonal prediction model, the Forecast-oriented Low Ocean Resolution model (FLOR; Vecchi et al., 2014), developed at the National Oceanic and Atmospheric Administration Geophysical Fluid Dynamics Laboratory (NOAA/GFDL). Pu and Ginoux (2017) found that surface wind, land surface bareness, and precipitation are key controlling factors affecting the interannual variations in dustiness in the United States, which statistically explain about 49–88% of the variances of dust event frequency over the southwestern United States and Great Plains during the recent decade. Using the regression model that reveals the relative importance of the controlling factors spatially and the controlling factors predicted by FLOR with 1 December initial conditions, we examine the capability of predicting springtime dustiness in major dusty regions in the United States. The potential sources of predictability are also discussed by comparing the above method with a one-season-lead regression model.

2. Data and Methodology

2.1. Data

Dust optical depth (DOD) describes the column integrated optical depth due to the extinction of dust. Daily DOD is retrieved from Moderate Resolution Imaging Spectroradiometer (MODIS) Deep Blue aerosol products (collection 6.0). Retrieval methods and estimated errors can be found in detail from Ginoux et al. (2012) and Pu and Ginoux (2018). MODIS DOD data have been used to study dust sources (Baddock et al., 2016; Ginoux et al., 2012), dust variations in the Middle East and United States (Pu & Ginoux, 2016, 2017), and model inter-comparison (Pu & Ginoux, 2018). Daily DOD derived from Aqua satellite products on a 0.1° by 0.1° grid from 2003 to 2016 is used in this study.

Dust event frequency is calculated by dividing the number of dusty days, that is, days when daily DOD is greater than one standard deviation (over 2004-2016), in each season to the total number of days in the season. This variable is used to quantify local dustiness. The results and conclusions would not change much if the frequency of occurrence (Ginoux et al., 2012) is used to quantify dustiness, that is, defining a dusty day as days when daily DOD is greater than a threshold, for example, DOD $\geq$ 0.02 (Pu et al., 2019).

10.1029/2019GL083703

Main dust sources in the United States are located over the southwestern and central United States (Ginoux et al., 2012). We therefore focus our analysis over these regions. Two averaging boxes, the southwestern United States (32–42°N, 105–124°W) and the Great Plains (25–49°N, 95–105°W), are defined following Pu and Ginoux (2017) to cover major dust sources. In the Great Plains, we further examined dustiness in the southern Great Plains (25–38°N, 95–105°W) and northern Great Plains (38–49°N, 95–105°W).

In addition to local sources, Asian dust has been found over the western United States in spring (e.g., Creamean et al., 2014; Yu et al., 2012) and African dust over the southeastern United States during the summer (e.g., Perry et al., 1997; Prospero, 1999). Since DOD is a column-integrated variable that does not distinguish local dust from remotely transported dust, in this study we do not separate local and transported dust as well, but focus on overall dustiness.

Surface wind, precipitation, and bareness are identified as key variables that affect the overall dustiness in the United States in the present climate (Pu & Ginoux, 2017). These factors have also been found by earlier studies to affect the emission and transportation of dust (e.g., Fécan et al., 1999; Gillette & Passi, 1988; Zender & Kwon, 2005). For instance, surface wind can lift dust from the bare surface to the atmosphere and transport it away from the source regions, while precipitation can remove small particles by scavenging and also increase soil moisture and enhance soil cohesion to prevent wind erosion. Vegetation coverage, on the other hand, can reduce near-surface wind by increasing surface roughness and also sustain soil moisture (e.g., Raupach, 1994; Zender et al., 2003).

Surface 10-m wind speed from the ERA-Interim (Dee et al., 2011), precipitation from the NOAA Precipitation Reconstruction over Land [PRECL; Chen et al., 2002], and leaf area index (LAI) from Advanced Very High Resolution Radiometer (AVHRR) satellite retrieval (Claverie et al., 2014; Claverie et al., 2016) are used to construct the regression model and validate FLOR predictions. These datasets have been used to examine the connection between dustiness and its dominant controlling factors in the United States and globally (Pu & Ginoux, 2017, 2018). Details about these datasets can be found in Text S1 in the supporting information. Bareness is defined following Evans et al. (2016) as Bareness = exp(-1×LAI). High value of bareness indicates low vegetation coverage, and vice versa.

2.2. Prediction Based on FLOR Ensemble Output and a Regression Model

The dust event frequency is predicted at each grid point on a 1.0° by 1.0° resolution as the following:

$$\text{Dust event frequency} = R_P \times P_F + R_V \times V_F + R_B \times B_F + C \tag{1}$$

where R_P, R_V, and R_B, and C are springtime regression coefficients of precipitation, surface wind, and bareness, and a constant value, respectively, from Pu and Ginoux (2017). The regression coefficients are obtained by regressing DOD onto standardized observational controlling factors in the same season. Details about the coefficients in each season can be found in Pu and Ginoux (2017). P_F, V_F, and B_F are standardized precipitation, surface wind, and bareness calculated from FLOR ensemble predictions. Since spring is one of the primary dust seasons in the United States, we use the controlling factors predicted by FLOR (i.e., precipitation, surface wind, and bareness) in spring, which is initialized on 1 December, to examine dust prediction capability of one season ahead.

FLOR is one of GFDL's present real-time seasonal prediction models and one of the North American Multimodel Ensemble [NMME; Kirtman et al., 2014] models that provide operational seasonal-to-interannual predictions. The atmosphere and land components of FLOR are from the GFDL Coupled Model version 2.5 [CM2.5; Delworth et al., 2012] with a horizontal resolution of about 50 km and totally 32 vertical levels. The ocean and sea ice components are developed from the GFDL Coupled Model version 2.1 [CM2.1; Delworth et al., 2006; Gnanadesikan et al., 2006; Wittenberg et al., 2006], with a horizontal resolution of about 100 km and 50 vertical layers. FLOR shows skill in seasonal prediction of different variables in the tropics and extratropics (Vecchi et al. 2014; Jia et al., 2015; Kapnick et al., 2018; Yang et al., 2015; Yang et al., 2018).

Two groups of FLOR ensemble simulations, En1 and En2, are used, each containing 12 members integrated for 12 months. Details about initial conditions in En1 and En2 can be found in Text S2. The setting of En1 is the same as that used by FLOR in the NMME. Note that monthly LAI in this group has no interannual

10.1029/2019GL083703

variations and corresponds a model simulation. Therefore, the prediction using En1 output only considers the contribution of surface wind and precipitation to the variations in dustiness.

Settings in En2 are the same as En1 except (1) the atmosphere and land initial conditions are from a FLOR simulation nudged toward reanalysis and observations, instead of from an Atmospheric Model Intercomparison Project (AMIP)-type ensemble simulation as in En1 (see Text S2 for details), and (2) LAI in En2 contains interannual variations and is identical for all the ensemble members. The atmosphere and land initial conditions in En2 are considered to be more realistic than that in En1 due to the nudging process. It is thus found the predictive skill in En2 is higher than En1 for United States summer temperature (Jia et al., 2016) and winter precipitation pattern over the western United States (Yang et al., 2018).

The retrospective predictions from both En1 and En2 from 2003 to 2016 are used. All the monthly variables from FLOR are interpolated to a 1.0° by 1.0° grid to be consistent with the regression model. We mainly focus on predicting the anomalies of dust event frequency, that is, the interannual variations in dustiness driven by the variations in the controlling factors (P_F, V_F, and B_F). This reduces the uncertainties associated with the constant value C in the regression model (equation (1)).

2.3. A one-season-lead regression model

To explore the sources of predictability, we also develop a one-season-lead regression model based on observational data alone. The multiple linear regression coefficients are determined by regressing DOD in the current season onto standardized surface wind, bareness, and precipitation in the preceding season. The regression coefficients and observed controlling factors in December-January-February (DJF) are used to reconstruct dustiness in March-April-May (MAM).

3. Results

3.1. Seasonal Prediction From the Regression Model and FLOR Output

Figures 1a and 1b show dust event frequency from MODIS (blue) and the prediction using the regression model and variables predicted by FLOR En1 ensemble mean (orange) for MAM, averaged over the southwestern United States and the Great Plains. The grey shading shows the range of the prediction from 12 ensemble members. Over the southwestern United States, the dustiness peaks during 2007-2008 and 2012-2013 in MODIS, largely associated with California droughts from 2007 to 2009 and from late 2011 to 2016 (also extending to early 2017; Seager et al., 2015; Ullrich et al., 2018; Wei et al., 2016; Xiao et al., 2017). Such a connection between droughts and increased dustiness in the United States is also noticed by Pu and Ginoux (2017). The prediction using En1 output largely misses these maxima of dustiness and overall has a negative correlation with MODIS (Figure 1a).

Over the Great Plains, the dust event frequency peaks around 2011 to 2012 in MODIS (Figure 1b), corresponding to the severe droughts in the southern Great Plains in 2011 (e.g., Fernando et al., 2016; Pu et al., 2016; Seager et al., 2014) and over the central United States in 2012 (e.g., Hoerling et al., 2014; Seager & Hoerling, 2014). In addition to precipitation deficit, enhanced surface wind and reduced bareness also contribute to the increase in dustiness during 2011-2012 in the Great Plains (Pu & Ginoux, 2017). A secondary peak in 2008 is largely associated with the dry condition over southern Texas from 2008 to 2009 (McRoberts & Nielsen-Gammon, 2012; Miller & Shank, 2013; Nielsen-Gammon & McRoberts, 2009). The prediction largely captures these maxima but overestimates dustiness from 2004 to 2007. The correlation between the prediction using En1 ensemble mean and MODIS is 0.82 from 2004 to 2016, indicating that the prediction statistically explained about 68% variances of dust event frequency.

When the output from En2 ensemble is used, the interannual variations of dust event frequency is better captured in both regions, with correlations of 0.79 and 0.84 for the southwestern United States and the Great Plains, respectively (Figures 1c and 1d). However, over the southwestern United States, magnitudes of the anomalies are still underestimated.

Why do predictions with En2 ensemble perform better than those of En1? The differences between En1 and En2 ensemble means can be largely attributed to the different land and atmosphere initial conditions. Land initial conditions, such as soil moisture, which has a memory up to several months (e.g., Entin et al., 2000; Koster et al., 2004; Koster et al., 2011), are critical for seasonal prediction of temperature and precipitation

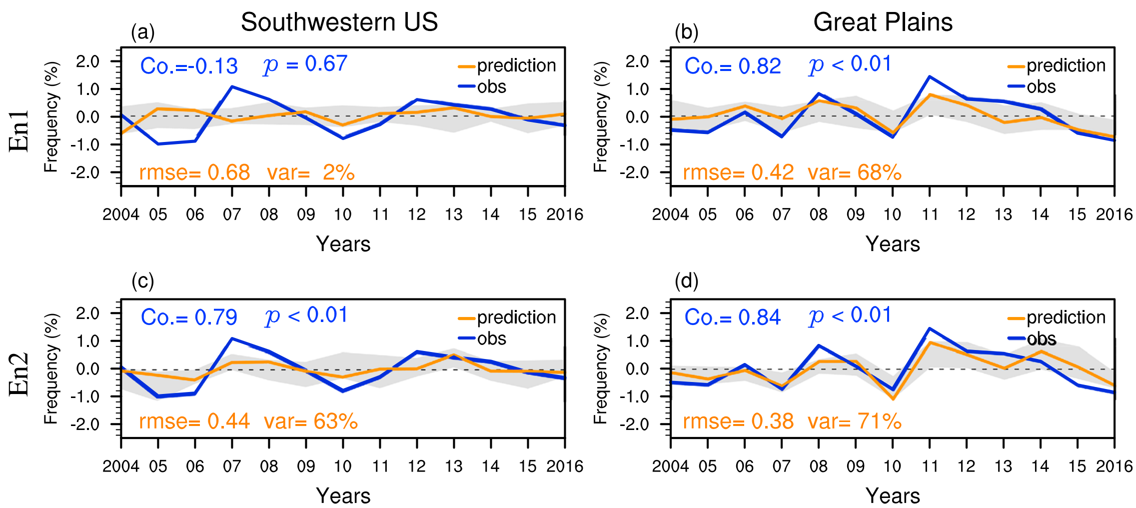

Figure 1. Regional averaged dust event frequency (anomalies) using output from (a and b) En1 and (c and d) En2 ensembles in (a), (c) the southwestern United States (32–42°N, 105–124°W), and (b and d) the Great Plains (25–49°N, 95–105°W) for MAM. Results from Moderate Resolution Imaging Spectroradiometer (MODIS) and the prediction using ensemble means are plotted in blue and orange lines, respectively. The grey shading indicates the range of the predictions from 12 ensemble members.

(e.g., Jia et al., 2016; Koster et al., 2011; Seneviratne et al., 2010; Yang et al., 2018). Information of low-frequency planetary waves (Shukla, 1981) in the atmospheric initial conditions is also an important source for predictability. More realistic land and atmosphere initial conditions in En2 thus improve precipitation and surface wind predictions over the southwestern United States and central Great Plains in spring and consequently improve the prediction of precipitation or surface wind induced variations in dustiness in the Southwest and the northern Great Plains (Figure S1 and Text S3 in the supporting information).

We also tested the prediction skill by combining the predicted controlling factors from En1 and En2 into one big ensemble (i.e., with 24 ensemble members), and the results are not overall better than using En2 alone (see Text S4 and Figure S2 for details).

3.2. Case Study

In addition to testing the prediction skill of regional means, we also examine the spatial pattern of the predicted dustiness anomaly. Two case studies are selected: (1) one year when both the Southwest and Great Plains show negative anomaly of dust event frequency, 2010, and (2) a period when the dustiness in the Great Plains is largely enhanced, 2011-2013 (Figure 1). Predicted anomalies for each year from 2004 to 2016 are shown in Figure S3.

Figure 2a shows the climatology of dust event frequency from MODIS in MAM. The high-frequency values are largely located over California and Arizona in the southwestern United States and over Texas, Kansas, and Nebraska in the Great Plains. In 2010, both the Southwest and the Great Plains show a reduced dustiness in MODIS (Figure 2b). The spatial pattern over the Great Plains is better captured when using the En2 ensemble mean, although the magnitude is overestimated over eastern Texas (Figures 2c and 2d). The negative anomalies over southern California and western Arizona are however not captured (Figure 2d), largely due to the misrepresentation of the variations in bareness (Figure S4d). As revealed by the En2 variables, such an overall reduction of dustiness over the Great Plains is largely contributed by variations in surface wind, with precipitation over the western to southern Great Plains and bareness in the central to southern Great Plains playing important roles (Figures S4b-S4d).

During 2011-2013, spring dustiness increased over the southwestern Great Plains, southern California, and western Arizona but decreased over central California and northeastern Great Plains (Figure 2e). Both predictions using the En1 and En2 ensembles miss the dipole anomalies in California, possibly due to biases in regional circulation and hydroclimate associated with spatial resolution in FLOR (Kapnick et al., 2018),

10.1029/2019GL083703

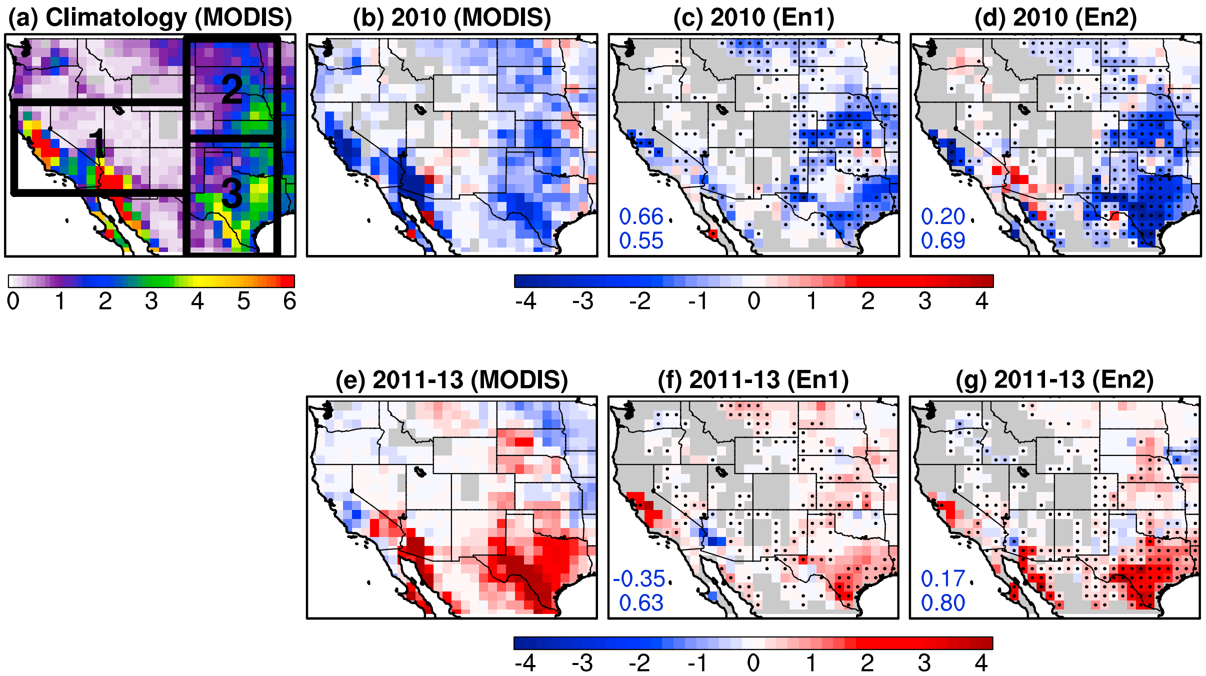

Figure 2. (a) Climatology (2004-2016) of dust event frequency (%) in March-April-May (MAM), and anomaly (with reference to the climatology; %) in 2010 from (b) Moderate Resolution Imaging Spectroradiometer (MODIS), (c) prediction with En1 ensemble, (d) prediction with En2 ensemble, and anomalies averaged between 2011 and 2013 from (e) MODIS, (f) prediction with En1, and (g) prediction with En2. The dotted area indicates that at least eight out of the 12 ensemble members show the same sign as MODIS anomalies. Missing values are shaded in grey. The black boxes denote the averaging areas over the southwestern United States (box 1) and northern (box 2) and southern Great Plains (box 3). Pattern correlations (uncentered) between the predictions and MODIS over the southwestern United States (first) and the Great Plains (second) are shown in bottom left in blue.

although positive anomalies over the Great Plains are largely captured (Figures 2f and 2g). The increases in dust event frequency over the southern to central Great Plains are contributed by all the controlling factors (Figures S4f-S4h).

3.3. Role of Land Surface Bareness

Since En1 ensemble does not include the interannual variations in surface bareness (or LAI), here we further examine the influence of bareness on seasonal dust prediction by comparing predictions using different controlling factors from FLOR ensembles (Figure 3). The correlations and root-mean-square error of each prediction are shown in Table S1 in the supporting information.

More than 65% of the variances are explained over the southern Great Plains and the Great Plains by using only precipitation and surface wind from En1 ensemble (Figure 3, first column). When including bareness from En2 ensemble (Figure 3, third column), higher variances of dustiness are explained over the Great Plains. This is consistent with Pu and Ginoux (2017), who found bareness plays an important role in the variations in dustiness over the western and part of central Great Plains.

For predictions using En2 ensemble, including the interannual variations in bareness increases the explained variances from 15 to 63% in the southwestern United States (Figure 3, fourth and second columns), although explained variances are slightly reduced over the southern Great Plains, likely due to the misrepresentation of the interannual variations in bareness in this region.

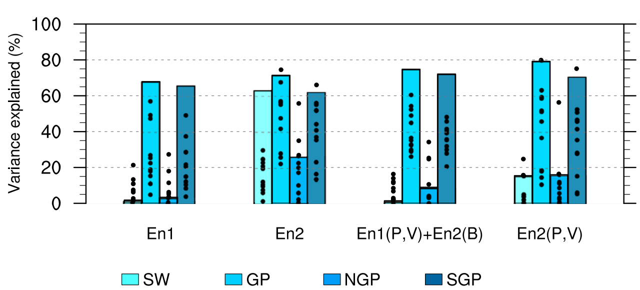

Figure 3. Variances (%) of March-April-May dust event frequency explained by predictions using different combination of Forecast-Oriented Low Ocean Resolution (FLOR) ensemble variables, from left to right: En1 ensemble, En 2 ensemble, precipitation and surface wind from En1 ensemble and bareness from En2, precipitation and surface wind from En2. Different color indicates different averaging regions: the southwestern United States (SW), the Great Plains (GP), the northern Great Plains (NGP), and the southern Great Plains (SGP). P, V, and B denote precipitation, surface wind, and bareness, respectively. The black dots denote results from each ensemble member.

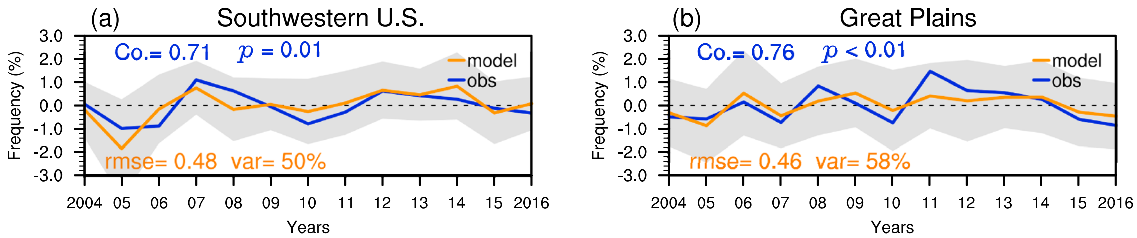

Figure 4. Regional averaged dust event frequency (anomalies) (a) in the southwestern United States and (b) the Great Plains in March-April-May from Moderate Resolution Imaging Spectroradiometer (MODIS; obs) and the reconstruction using one-season-lead regression model and observed precipitation, bareness, and surface wind speed in December-January-February (model) are shown in blue and orange lines, respectively. The grey shading indicates the 90% confidence interval (*t* test).

To quantify the role of bareness bias on prediction skill, we repeat our analysis with observed bareness from AVHRR (Figure S5). The explained variances are much better captured in the En1 case (increase more than 20%) and over the Great Plains in the En2 case (increase ~15%) with observed bareness. The magnitude of interannual variations in dustiness over the southwestern United States is also better represented in the En2 case (not shown). This indicates that bareness plays an essential role in seasonal dust prediction, and improvements in LAI predictions in addition to precipitation and surface wind prediction may further enhance the prediction skill of dustiness.

3.4. One-Season-Lead Regression Model

The regression model by Pu and Ginoux (2017) is developed by relating dust event frequency to concurrent controlling factors. Is it possible to use observed variations in the controlling factors one season ahead to predict the dustiness in the current season? We first calculate regression coefficients using wintertime controlling factors and springtime dust event frequency. Over the southwestern United States and Great Plains, it is mainly bareness and precipitation (and consequently soil moisture) in winter that are likely to affect the springtime dustiness, while surface wind plays a minor role over a small portion of western Arizona and over parts of the central Great Plains (Figure S6a). In general, the area with statistically significant regression coefficients is less than that in the concurrent springtime regression (Figure S6b), indicating weaker influences of wintertime controlling factors on springtime dustiness than springtime controlling factors.

Figure 4 shows reconstructed springtime dust event frequency (orange) using the coefficients from the one-season-lead regression model in MAM and observed controlling factors in DJF. The interannual variations in dustiness is partially represented, and about 58% of the variances over the Great Plains and 50% over the southwestern United States are explained, much lower than that captured by observed springtime controlling factors (76-79%; Pu & Ginoux, 2017). Predictions made by the one-season-lead regression model using DJF observations as predictors show little skill (Figure S7).

4. Discussion and Conclusions

Building upon Pu and Ginoux (2017), who found that interannual variations in dustiness in the United States are largely controlled by variations in local surface wind speed, precipitation, and bareness, we examine the capability of seasonal dust prediction in the United States by using key controlling factors predicted by the FLOR seasonal prediction model developed at the NOAA GFDL and an observation-constrained regression model (Pu & Ginoux, 2017). It is found that using predicted springtime surface wind and precipitation from the FLOR ensemble initialized at 1 December, the regression model can largely capture the interannual variations of dust event frequency in the Great Plains during MAM, explaining about 68% of the variances from 2004 to 2016. When FLOR is initialized with more realistic atmosphere and land initial conditions, both surface wind and precipitation over the southwestern United States and precipitation in the northern Great Plains are better predicted; together with the interannual variations of bareness, the regression model is able to explain 71% of variance of springtime dust event frequency in the Great Plains and 63% of the variances in the southwestern United States.

Such predictability of dustiness, that is, from 1 December to MAM, lies in both the regression model, which provides spatial information about the relative importance of each of the local controlling factors and the prediction skill from FLOR. In FLOR En1 ensemble, the ocean and sea ice components of the model are initialized from the assimilated data, which contain information of observed sea surface temperature and sea ice in December. In the En2 ensemble, additional skill is obtained from the more realistic atmosphere and land initial conditions. Here wintertime sea surface temperature, sea ice, atmosphere, and land initial conditions are important sources of predictability for FLOR to skillfully predict the variations in precipitation and surface wind speed in the United States about 3 to 6 months later. Seasonal dust prediction skill is overall lower in the Southwest than the Great Plains, likely due to missing values in the regression model and difficulties for FLOR to capture the hydro-climate processes in mountainous area with current horizontal resolution.

On the other hand, a one-season-lead regression model using observed precipitation, surface wind, and bareness in DJF shows lower skill in reproducing springtime dustiness. Wintertime precipitation and bareness affect dustiness in spring, but the overall influences are weaker than that from the springtime controlling factors.

This study is an early attempt to explore the capability of seasonal prediction of dust, and findings here will provide useful information for building a seasonal dust prediction system. The proposed prediction method has some limitations. The regression model used here is based on a relatively short time period of DOD; thus, information regarding to low-frequency (e.g., decadal) variations in dust is not included. Other factors and mechanisms (e.g., anthropogenic activities) in addition to surface wind, bareness, and precipitation on the interannual variations in dustiness are not included. How other large-scale remote factors, such as El Niño-Southern Oscillation, may affect local factors and influence seasonal dust predictability will need further investigation. Incorporating an interactive dust scheme into seasonal prediction models will likely provide a more physical-based prediction and potentially benefit predictions of other variables by including the radiative forcing from dust (e.g., Pérez et al., 2006). Nonetheless, despite the advantages of interactive dust schemes, information on soil characteristics in arid regions is sparse and dust emission parameterizations may be insufficiently constrained making statistical models still quite useful tools. Going beyond statistical models by using Artificial Intelligence and Machine Learning algorithms offers another new path to improve skills for seasonal dust prediction.

Data Availability

The MODIS Deep Blue aerosol products were acquired from the Level-1 and Atmosphere Archive and Distribution System (LAADS) Distributed Active Archive Center (DAAC), located in the Goddard Space Flight Center in Greenbelt, Maryland (https://ladsweb.nascom.nasa.gov/). PRECL precipitation data are provided by the NOAA/OAR/ESRL PSD, Boulder, Colorado, USA, from their website at https://www.esrl.noaa.gov/psd/data/gridded/data.precl.html. ERA-Interim is downloaded from https://www.ecmwf.int/en/forecasts/datasets/reanalysis-datasets/era-interim. AVHRR leaf area index is downloaded from https://data.nodc.noaa.gov/cgi-bin/iso?id=gov.noaa.ncdc:C00898.

Acknowledgments
This research is supported by NOAA and Princeton University's Cooperative Institute for Climate Science (NA14OAR4320752) and NASA under grant NNH14ZDA001N-ACMAP and NNH16ZDA001N-MAP. The authors would like to thank Sergey Malyshev for his great help in understanding land model settings and Nathaniel Johnson and Salvatore Pascale for their valuable comments on the early version of this manuscript.The insightful comments from the two anonymous reviewers improved the paper.

References

Baddock, M. C., Ginoux, P., Bullard, J. E., & Gill, T. E. (2016). Do MODIS-defined dust sources have a geomorphological signature? *Geophysical Research Letters*, *43*, 2606–2613. https://doi.org/10.1002/2015GL067327

Chen, M. Y., Xie, P. P., Janowiak, J. E., & Arkin, P. A. (2002). Global land precipitation: A 50-yr monthly analysis based on gauge observations. *Journal of Hydrometeorology*, *3*(3), 249–266.

Christensen, J. H. (1997). The Danish Eulerian hemispheric model - A three-dimensional air pollution model used for the Arctic. *Atmospheric Environment*, *31*(24), 4169–4191.

Claverie, M., Matthews, J. L., Vermote, E. F., & Justice, C. O. (2016). A 30+ year AVHRR LAI and FAPAR Climate Data Record: Algorithm description and validation. *Remote Sensing-Basel*, *8*(3).

Claverie, M., Vermote, E., & Program, N. C. (2014). NOAA Climate Data Record (CDR) of leaf area index (LAI) and fraction of absorbed photosynthetically active radiation (FAPAR), Version 4,, edited by N. N. C. D. Center.

Cook, B. I., Miller, R. L., & Seager, R. (2008). Dust and sea surface temperature forcing of the 1930s "Dust Bowl" drought. *Geophysical Research Letters*, *35*, L08710. https://doi.org/10.1029/2008GL033486

Cook, B. I., Miller, R. L., & Seager, R. (2009). Amplification of the North American "Dust Bowl" drought through human-induced land degradation. *Proceedings of the National Academy of Sciences of the United States of America*, *106*(13), 4997–5001.

Cook, B. I., Seager, R., Miller, R. L., & Mason, J. A. (2013). Intensification of North American megadroughts through surface and dust aerosol forcing. *Journal of Climate*, *26*(13), 4414–4430.

Creamean, J. M., Spackman, J. R., Davis, S. M., & White, A. B. (2014). Climatology of long-range transported Asian dust along the West Coast of the United States. *Journal of Geophysical Research: Atmospheres*, *119*, 12,171–12,185. https://doi.org/10.1002/2014JD021694

Crooks, J. L., Cascio, W. E., Percy, M. S., Reyes, J., Neas, L. M., & Hilborn, E. D. (2016). The association between dust storms and daily non-accidental mortality in the United States, 1993-2005. *Environmental Health Perspectives*, *124*(11), 1735–1743.

Dee, D. P., Uppala, S. M., Simmons, A. J., Berrisford, P., Poli, P., Kobayashi, S., et al. (2011). The ERA-Interim reanalysis: Configuration and performance of the data assimilation system. *Quarterly Journal of the Royal Meteorological Society*, *137*(656), 553–597. https://doi.org/10.1002/qj.828

Delworth, T. L., Broccoli, A. J., Rosati, A., Stouffer, R. J., Balaji, V., Beesley, J. A., et al. (2006). GFDL's CM2 global coupled climate models. Part I: Formulation and simulation characteristics. *Journal of Climate*, *19*(5), 643–674. https://doi.org/10.1175/JCLI3629.1

Delworth, T. L., Rosati, A., Anderson, W., Adcroft, A. J., Balaji, V., Benson, R., et al. (2012). Simulated climate and climate change in the GFDL CM2.5 high-resolution coupled climate model. *Journal of Climate*, *25*(8), 2755–2781. https://doi.org/10.1175/JCLI-D-11-00316.1

Doblas-Reyes, F. J., Garcia-Serrano, J., Lienert, F., Biescas, A. P., & Rodrigues, L. R. L. (2013). Seasonal climate predictability and forecasting: status and prospects. *WIREs Climate Change*, *4*(4), 245–268.

Entin, J. K., Robock, A., Vinnikov, K. Y., Hollinger, S. E., Liu, S. X., & Namkhai, A. (2000). Temporal and spatial scales of observed soil moisture variations in the extratropics. *Journal of Geophysical Research*, *105*(D9), 11,865–11,877.

Evans, S., Ginoux, P., Malyshev, S., & Shevliakova, E. (2016). Climate-vegetation interaction and amplification of Australian dust variability. *Geophysical Research Letters*, *43*, 11,823–11,830. https://doi.org/10.1002/2016GL071016

Fécan, F., Marticorena, B., & Bergametti, G. (1999). Parametrization of the increase of the aeolian erosion threshold wind friction velocity due to soil moisture for arid and semi-arid areas. *Annales Geophysicae*, *17*(1), 149–157.

Fernando, D. N., Mo, K. C., Fu, R., Pu, B., Bowerman, A., Scanlon, B. R., et al. (2016). What caused the spring intensification and winter demise of the 2011 drought over Texas? *Climate Dynamics*, *47*(9-10), 3077–3090. https://doi.org/10.1007/s00382-016-3014-x

Gao, T., Zhang, X. B., Li, Y. P., Wang, H. M., Xiao, S. J., Wulan, & Teng, Q. B. (2009). Potential predictors for spring season dust storm forecast in Inner Mongolia, China. *Theoretical and Applied Climatology*, *97*(3-4), 255–263.

Gao, T., Zhang, X. B., & Wulan (2010). A seasonal forecast scheme for spring dust storm predictions in Northern China. *Meteorological Applications*, *17*(4), 433–441.

Giannadaki, D., Pozzer, A., & Lelieveld, J. (2014). Modeled global effects of airborne desert dust on air quality and premature mortality. *Atmospheric Chemistry and Physics*, *14*(2), 957–968.

Gillette, D. A., & Passi, R. (1988). Modeling dust emission caused by wind erosion. *Journal of Geophysical Research*, *93*(D11), 14,233–14,242.

Ginoux, P., Prospero, J. M., Gill, T. E., Hsu, N. C., & Zhao, M. (2012). Global-scale attribution of anthropogenic and natural dust sources and their emission rates based on MODIS Deep Blue aerosol products. *Reviews of Geophysics*, *50*, RG3005. https://doi.org/10.1029/2012RG000388

Gnanadesikan, A., Dixon, K. W., Griffies, S. M., Balaji, V., Barreiro, M., Beesley, J. A., et al. (2006). GFDL's CM2 global coupled climate models. Part II: The baseline ocean simulation. *Journal of Climate*, *19*(5), 675–697. https://doi.org/10.1175/JCLI3630.1

Goudie, A. S. (2009). Dust storms: Recent developments. *Journal of Environmental Management*, *90*(1), 89–94.

Hand, J. L., Gill, T. E., & Schichtel, B. A. (2017). Spatial and seasonal variability in fine mineral dust andcoarse aerosol mass at remote sites across the United States, *Journal of Geophysical Research: Atmospheres*, *122*, 3080-3097.

Haustein, K., Pérez, C., Baldasano, J. M., Jorba, O., Basart, S., Miller, R. L., et al. (2012). Atmospheric dust modeling from meso to global scales with the online NMMB/BSC-Dust model—Part 2: Experimental campaigns in Northern Africa. *Atmospheric Chemistry and Physics*, *12*(6), 2933–2958. https://doi.org/10.5194/acp-12-2933-2012

Hoerling, M., Eischeid, J., Kumar, A., Leung, R., Mariotti, A., Mo, K., et al. (2014). Causes and predictability of the 2012 Great Plains drought. *Bulletin of the American Meteorological Society*, *95*(2), 269–282.

Jia, L. W., Vecchi, G. A., Yang, X. S., Gudgel, R. G., Delworth, T. L., Stern, W. F., et al. (2016). The roles of radiative forcing, sea surface temperatures, and atmospheric and land initial conditions in US summer warming episodes. *Journal of Climate*, *29*(11), 4121–4135.

Jia, L. W., Yang, X., Vecchi, G. A., Gudgel, R. G., Delworth, T. L., Rosati, A., et al. (2015). Improved seasonal prediction of temperature and precipitation over land in a high-resolution GFDL climate model. *Journal of Climate*, *28*(5), 2044–2062. https://doi.org/10.1175/JCLI-D-14-00112.1

Kallos, G., Papadopoulos, A., Katsafados, P., & Nickovic, S. (2006). Transatlantic Saharan dust transport: Model simulation and results. *Journal of Geophysical Research*, *111*, D09204. https://doi.org/10.1029/2005JD006207

Kapnick, S. B., Yang, X. S., Vecchi, G. A., Delworth, T. L., Gudgel, R., Malyshev, S., et al. (2018). Potential for western US seasonal snowpack prediction. *Proceedings of the National Academy of Sciences of the United States of America*, *115*(6), 1180–1185.

Kirtman, B. P., Min, D., Infanti, J. M., Kinter, J. L. III, Paolino, D. A., Zhang, Q., et al. (2014). The North American multimodel ensemble phase-1 seasonal-to-interannual prediction; Phase-2 toward developing intraseasonal prediction. *Bulletin of the American Meteorological Society*, *95*(4), 585–601. https://doi.org/10.1175/BAMS-D-12-00050.1

Kolivras, K. N., & Comrie, A. C. (2004). Climate and infectious disease in the southwestern United States. *Progress in Physical Geography*, *28*(3), 387–398.

Koster, R. D., Mahanama, S. P. P., Yamada, T. J., Balsamo, G., Berg, A. A., Boisserie, M., et al. (2011). The second phase of the global land-atmosphere coupling experiment: Soil moisture contributions to subseasonal forecast skill. *Journal of Hydrometeorology*, *12*(5), 805–822. https://doi.org/10.1175/2011JHM1365.1

Koster, R. D., Suarez, M. J., Liu, P., Jambor, U., Berg, A., Kistler, M., et al. (2004). Realistic initialization of land surface states: Impacts on subseasonal forecast skill. *Journal of Hydrometeorology*, *5*(6), 1049–1063.

McRoberts, D. B., & Nielsen-Gammon, J. W. (2012). The use of a high-resolution standardized precipitation index for drought monitoring and assessment. *Journal of Applied Meteorology and Climatology*, *51*(1), 68–83.

Miller, S. A., & Shank, G. C. (2013). Influence of severe drought conditions on chromophoric dissolved organic matter dynamics in south Texas coastal waters. *Estuarine, Coastal and Shelf Science*, *117*, 219–226.

Nielsen-Gammon, J., & McRoberts, B. (2009). An assessment of the meteorological severity of the 200809 Texas drought through July 2009Rep., Office of the State Climatologist, Texas A&M University (https://climatexas.tamu.edu/files/august_2009_drought.pdf).

Painter, T. H., Deems, J. S., Belnap, J., Hamlet, A. F., Landry, C. C., & Udall, B. (2010). Response of Colorado River runoff to dust radiative forcing in snow. *Proceedings of the National Academy of Sciences of the United States of America*, *107*(40), 17,125–17,130.

Painter, T. H., Skiles, S. M., Deems, J. S., Brandt, W. T., & Dozier, J. (2018). Variation in rising limb of Colorado River snowmelt runoff hydrograph controlled by dust radiative forcing in Snow. *Geophysical Research Letters*, *45*, 797–808. https://doi.org/10.1002/2017GL075826

Pérez, C., Haustein, K., Janjic, Z., Jorba, O., Huneeus, N., Baldasano, J. M., et al. (2011). Atmospheric dust modeling from meso to global scales with the online NMMB/BSC-Dust model—Part 1: Model description, annual simulations and evaluation. *Atmospheric Chemistry and Physics*, *11*(24), 13,001–13,027. https://doi.org/10.5194/acp-11-13001-2011

Pérez, C., Nickovic, S., Pejanovic, G., Baldasano, J. M., & Ozsoy, E. (2006). Interactive dust-radiation modeling: A step to improve weather forecasts. *Journal of Geophysical Research*, *111*, D16206. https://doi.org/10.1029/2005JD006717

Pérez García-Pando, C., Stanton, M. C., Diggle, P. J., Trzaska, S., Miller, R. L., Perlwitz, J. P., et al. (2014). Soil dust aerosols and wind as predictors of seasonal meningitis incidence in Niger. *Environmental Health Perspectives*, *122*(7), 679–686. https://doi.org/10.1289/ehp.1306640

Perry, K. D., Cahill, T. A., Eldred, R. A., Dutcher, D. D., & Gill, T. E. (1997). Long-range transport of North African dust to the eastern United States. *Journal of Geophysical Research*, *102*(D10), 11,225–11,238.

Prospero, J. M. (1999). Long-range transport of mineral dust in the global atmosphere: Impact of African dust on the environment of the southeastern United States. *Proceedings of the National Academy of Sciences of the United States of America*, *96*(7), 3396–3403.

Pu, B., Fu, R., Dickinson, R. E., & Fernando, D. N. (2016). Why do summer droughts in the Southern Great Plains occur in some La Nina years but not others? *Journal of Geophysical Research: Atmospheres*, *121*, 1120–1137. https://doi.org/10.1002/2015JD023508

Pu, B., & Ginoux, P. (2016). The impact of the Pacific Decadal Oscillation on springtime dust activity in Syria. *Atmospheric Chemistry and Physics*, *16*(21), 13,431–13448.

Pu, B., & Ginoux, P. (2017). Projection of American dustiness in the late 21st century due to climate change. *Scientific Reports*, *7*.

Pu, B., & Ginoux, P. (2018). How reliable are CMIP5 models in simulating dust optical depth? *Atmospheric Chemistry and Physics*, *18*(16), 12,491–12,510.

Pu, B., Ginoux, P., Guo, H., Hsu, N. C., Kimball, J., Marticorena, B., et al. (2019). Retrieving the global distribution of threshold of wind erosion from satellite data and implementing it into the GFDL AM4.0/LM4.0 model. *Atmospheric Chemistry and Physics Discussions*, 1–74. https://doi.org/10.5194/acp-2019-223

Raupach, M. R. (1994). Simplified expressions for vegetation roughness length and zero-plane displacement as functions of canopy height and area index. *Boundary-Layer Meteorology*, *71*(1-2), 211–216.

Reid, J. S., Hyer, E. J., Prins, E. M., Westphal, D. L., Zhang, J., Wang, J., et al. (2009). Global monitoring and forecasting of biomass-burning smoke: Description of and lessons from the Fire Locating and Modeling of Burning Emissions (FLAMBE) Program. *IEEE Journal of Selected Topics in Applied Earth Observations and Remote Sensing*, *2*(3), 144–162.

Rubin, J. I., Reid, J. S., Hansen, J. A., Anderson, J. L., Collins, N., Hoar, T. J., et al. (2016). Development of the Ensemble Navy Aerosol Analysis Prediction System (ENAAPS) and its application of the Data Assimilation Research Testbed (DART) in support of aerosol forecasting. *Atmospheric Chemistry and Physics*, *16*(6), 3927–3951. https://doi.org/10.5194/acp-16-3927-2016

Schweitzer, M. D., Calzadilla, A. S., Salamo, O., Sharifi, A., Kumar, N., Holt, G., et al. (2018). Lung health in era of climate change and dust storms. *Environmental Research*, *163*, 36–42.

Seager, R., Goddard, L., Nakamura, J., Henderson, N., & Lee, D. E. (2014). Dynamical causes of the 2010/11 Texas-Northern Mexico Drought*. *Journal of Hydrometeorology*, *15*(1), 39–68.

Seager, R., & Hoerling, M. (2014). Atmosphere and ocean origins of North American droughts. *Journal of Climate*, *27*(12), 4581–4606.

Seager, R., Hoerling, M., Schubert, S., Wang, H. L., Lyon, B., Kumar, A., et al. (2015). Causes of the 2011-14 California drought*. *Journal of Climate*, *28*(18), 6997–7024.

Seneviratne, S. I., Corti, T., Davin, E. L., Hirschi, M., Jaeger, E. B., Lehner, I., et al. (2010). Investigating soil moisture-climate interactions in a changing climate: A review. *Earth Science Reviews*, *99*(3-4), 125–161.

Shukla, J. (1981). Dynamical Predictability of Monthly Means. *Journal of the Atmospheric Sciences*, *38*(12), 2547–2572.

Sohn, K. T. (2013). Statistical guidance on seasonal forecast of Korean dust days over South Korea in the springtime. *Advances in Atmospheric Sciences*, *30*(5), 1343–1352.

Tong, D. Q., Wang, J. X. L., Gill, T. E., Lei, H., & Wang, B. Y. (2017). Intensified dust storm activity and Valley fever infection in the southwestern United States. *Geophysical Research Letters*, *44*, 4304–4312. https://doi.org/10.1002/2017GL073524

Ullrich, P. A., Xu, Z., Rhoades, A. M., Dettinger, M. D., Mount, J. F., Jones, A. D., & Vahmani, P. (2018). California's drought of the future: A midcentury recreation of the exceptional conditions of 2012-2017. *Earth's Future*, *6*, 1568–1587. https://doi.org/10.1029/2018EF001007

Vecchi, G. A., Delworth, T., Gudgel, R., Kapnick, S., Rosati, A., Wittenberg, A. T., et al. (2014). On the seasonal forecasting of regional tropical cyclone activity. *Journal of Climate*, *27*(21), 7994–8016. https://doi.org/10.1175/JCLI-D-14-00158.1

Wei, J. F., Jin, Q. J., Yang, Z. L., & Dirmeyer, P. A. (2016). Role of ocean evaporation in California droughts and floods. *Geophysical Research Letters*, *43*, 6554–6562. https://doi.org/10.1002/2016GL069386

Westphal, D. L., Curtis, C. A., Liu, M., & Walker, A. L. (2009). Operational aerosol and dust storm forecasting, in WMO/GEO Expert Meeting on an International Sand and Dust Storm Warning System, in *IOP Conference Series Earth and Environmental Science*, edited, p. 012007.

Witek, M. L., Flatau, P. J., Quinn, P. K., & Westphal, D. L. (2007). Global sea-salt modeling: Results and validation against multicampaign shipboard measurements. *Journal of Geophysical Research*, *112*, D08215. https://doi.org/10.1029/2006JD007779

Wittenberg, A. T., Rosati, A., Lau, N. C., & Ploshay, J. J. (2006). GFDL's CM2 global coupled climate models. Part III: Tropical pacific climate and ENSO. *Journal of Climate*, *19*(5), 698–722.

Xiao, M., Koppa, A., Mekonnen, Z., Pagan, B. R., Zhan, S. A., Cao, Q. A., et al. (2017). How much groundwater did California's Central Valley lose during the 2012-2016 drought? *Geophysical Research Letters*, *44*, 4872–4879. https://doi.org/10.1002/2017GL073333

Yang, X. S., Jia, L. W., Kapnick, S. B., Delworth, T. L., Vecchi, G. A., Gudgel, R., et al. (2018). On the seasonal prediction of the western United States El Nino precipitation pattern during the 2015/16 winter. *Climate Dynamics*, *51*(9-10), 3765–3783.

Yang, X. S., Vecchi, G. A., Gudgel, R. G., Delworth, T. L., Zhang, S., Rosati, A., et al. (2015). Seasonal predictability of extratropical storm tracks in GFDL's high-resolution climate prediction model. *Journal of Climate*, *28*(9), 3592–3611. https://doi.org/10.1175/JCLI-D-14-00517.1

Yu, H. B., Remer, L. A., Chin, M., Bian, H. S., Tan, Q., Yuan, T. L., & Zhang, Y. (2012). Aerosols from overseas rival domestic emissions over North America. *Science*, *337*(6094), 566–569.

Zender, C. S., & Kwon, E. Y. (2005). Regional contrasts in dust emission responses to climate. *Journal of Geophysical Research*, *110*, D13201. https://doi.org/10.1029/2004JD005501

Zender, C. S., Newman, D., & Torres, O. (2003). Spatial heterogeneity in aeolian erodibility: Uniform, topographic, geomorphic, and hydrologic hypotheses. *Journal of Geophysical Research*, *108*(D17), 4543. https://doi.org/10.1029/2002JD003039

Zhao, C., Liu, X., & Leung, L. R. (2012). Impact of the Desert dust on the summer monsoon system over Southwestern North America. *Atmospheric Chemistry and Physics*, *12*(8), 3717–3731.

References From the Supporting Information

Chang, Y. S., Zhang, S. Q., Rosati, A., Delworth, T. L., & Stern, W. F. (2013). An assessment of oceanic variability for 1960-2010 from the GFDL ensemble coupled data assimilation. *Climate Dynamics*, *40*(3-4), 775–803.

Rienecker, M. M., Suarez, M. J., Gelaro, R., Todling, R., Bacmeister, J., Liu, E., et al. (2011). MERRA: NASA's Modern-Era Retrospective Analysis for Research and Applications. *Journal of Climate*, *24*(14), 3624–3648. https://doi.org/10.1175/JCLI-D-11-00015.1

Zhang, S., Harrison, M. J., Rosati, A., & Wittenberg, A. (2007). System design and evaluation of coupled ensemble data assimilation for global oceanic climate studies. *Monthly Weather Review*, *135*(10), 3541–3564.

Zhang, S., & Rosati, A. (2010). An inflated ensemble filter for ocean data assimilation with a biased coupled GCM. *Monthly Weather Review*, *138*(10), 3905–3931.